

Dark Matter Annihilation & 21 cm Cosmology

Laura Lopez Honorez

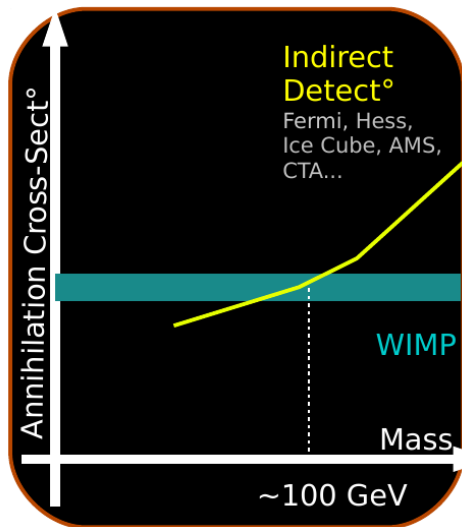
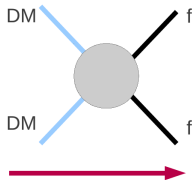


based on JCAP 1608 (2016) no.08, 004

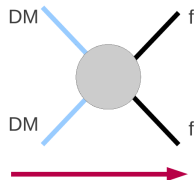
in collaboration with O. Mena, A. Moline, S. Palomares-Ruiz & A. C. Vincent.

IBS-Multidark-IPPP workshop: DM from aeV to ZeV
Lumley Castle, 21-15/11/2016

DM searches



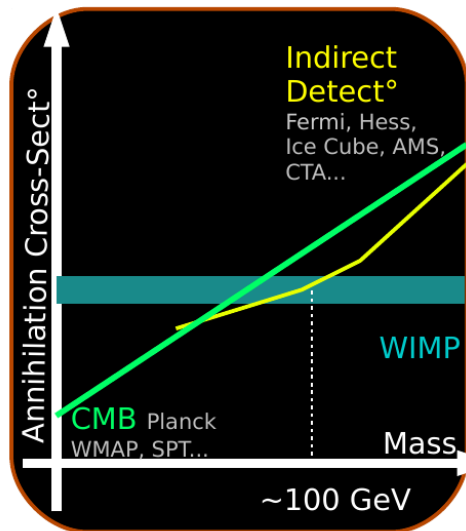
DM searches



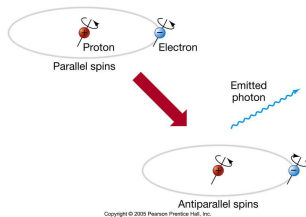
Cosmology probes have
already provided
constraints on DM
annihilation

IN THIS TALK:

**21 cm constraints on DM
annihilation**

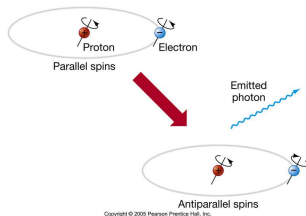


21 cm signal?

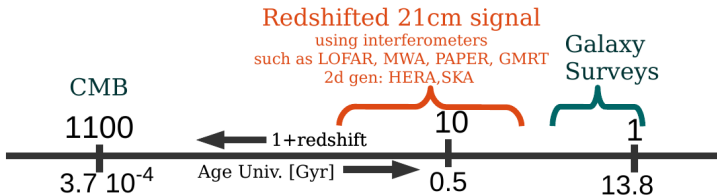


- Transitions between the two ground state energy levels of neutral hydrogen HI
↪ 21 cm photon ($\nu_0 = 1420$ MHz)

21 cm signal?



- Transitions between the two ground state energy levels of neutral hydrogen HI
 \rightsquigarrow 21 cm photon ($\nu_0 = 1420$ MHz)
- 21 cm photon from HI clouds during **dark ages & EoR** redshifted to $\nu \sim 100$ MHz
 \rightsquigarrow **new cosmology probe**

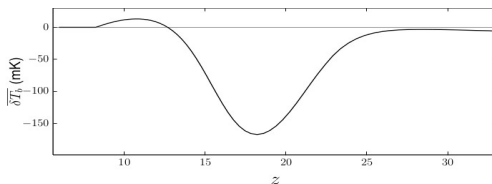


The observed brightness of a patch of HI relative to the CMB at $\nu = \nu_0/(1+z)$ is associated to the differential brightness temperature δT_b :

$$\delta T_b(\nu) \simeq 27 x_{\text{HI}} (1 + \delta_b) \left(1 - \frac{T_{\text{CMB}}}{T_S}\right) \left(\frac{1}{1 + H^{-1} \partial v_r / \partial r}\right) \left(\frac{1+z}{10}\right)^{1/2} \left(\frac{0.15}{\Omega_m h^2}\right)^{1/2} \left(\frac{\Omega_b h^2}{0.023}\right) \text{mK}$$

Fraction of neutral H

Spin temperature = excitation T of 21cm line

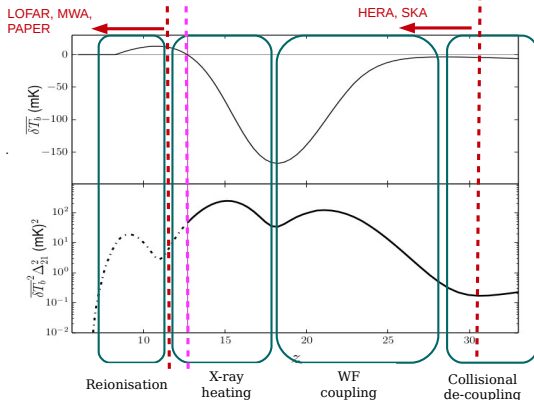


The observed brightness of a patch of HI relative to the CMB at $\nu = \nu_0/(1+z)$ is associated to the differential brightness temperature δT_b :

$$\delta T_b(\nu) \simeq 27 x_{\text{HI}} (1 + \delta_b) \left(1 - \frac{T_{\text{CMB}}}{T_S}\right) \left(\frac{1}{1 + H^{-1} \partial v_r / \partial r}\right) \left(\frac{1+z}{10}\right)^{1/2} \left(\frac{0.15}{\Omega_m h^2}\right)^{1/2} \left(\frac{\Omega_b h^2}{0.023}\right) \text{mK}$$

Fraction of neutral H

Spin temperature = excitation T of 21cm line



$$\langle \tilde{\delta}_{21}(\mathbf{k}, z) \tilde{\delta}_{21}^*(\mathbf{k}', z) \rangle \equiv (2\pi)^3 \delta^D(\mathbf{k} - \mathbf{k}') P_{21}(k, z) \quad \Delta_{21}^2(k, z) = \frac{k^3}{2\pi^2} P_{21}(k, z)$$

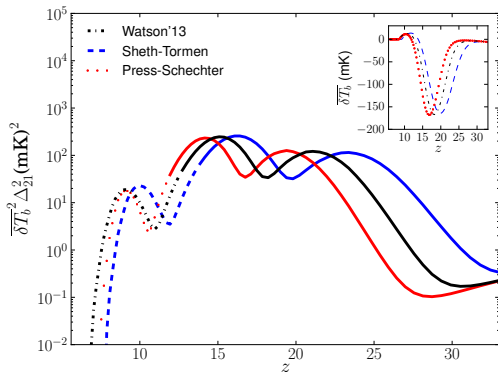
$$\delta_{21}(\mathbf{x}, z) = \delta T_b(\mathbf{x}, z) / \overline{\delta T_b(z)} - 1$$

Astro-params: halo mass function

For δT_b and Δ_{21} , we make use of 21cm Fast [Mesinger'10]

\rightsquigarrow dependence on halo mass function, T_{vir} , ζ_X , N_α . In particular, the ionization, heating and excitation critically depend on the fraction of mass collapsed in halos

$$f_{\text{coll}}(> M_{\text{vir}}) = \int_{M_{\text{vir}}} \frac{M}{\rho_0} \frac{dn(M, z)}{dM} dM,$$



- **PS:** underpredicts $\frac{dn(M, z)}{dM}$ at large M and z and overpredicts $\frac{dn(M, z)}{dM}$ at low M and z
- **ST:** default 21cmFast: slight overestimation compared to simu. at large z see e.g. Watson'13
- **W13:** our default

\rightsquigarrow PS \rightarrow W13 \rightarrow ST: astro sources switch on earlier

Energy *deposition* from DM annihilations

see previous work [Shchekinov'06, Furlanetto'06, Valdes'07, Chuzhoy'07, Cumberbatch'08, Natarajan'09, Yuan'09, Valdes'12, Evoli'14], see also [Chen'03, Hansen'03, Pierpaoli'03, Padmanabhan'05] for CMB

- What does DM annihilate into?:

- $f, \gamma, W, Z, \dots \rightsquigarrow e^+, e^-, \gamma$ using e.g. [Pythia, Mardon'09, PPPC4DMID]
- neutrinos \rightsquigarrow via EW corrections

Energy deposition from DM annihilations

see previous work [Shchekinov'06, Furlanetto'06, Valdes'07, Chuzhoy'07, Cumberbatch'08, Natarajan'09, Yuan'09, Valdes'12, Evoli'14], see also [Chen'03, Hansen'03, Pierpaoli'03, Padmanabhan'05] for CMB

• What does DM annihilate into?:

- $f, \gamma, W, Z, \dots \rightsquigarrow e^+, e^-, \gamma$ using e.g. [Pythia, Mardon'09, PPPC4DMID]
- neutrinos \rightsquigarrow via EW corrections

• Dark matter annihilation inject energy within the dark ages

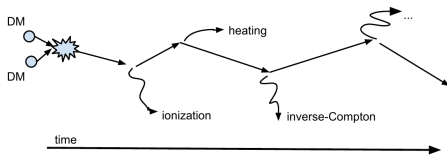


[image from A. Vincent]

Rate of energy injection/deposition into $c = \text{heat, ionization, excitation}$

$$\left(\frac{dE_c(\mathbf{x}, z)}{dt dV} \right)_{\text{deposited}}^{\text{smooth}} \equiv f_c(z) \left(\frac{dE(\mathbf{x}, z)}{dt dV} \right)_{\text{injected}}^{\text{smooth}} \equiv f_c(z) n_{DM}(z)^2 \frac{\langle \sigma v \rangle}{m_{DM}}$$

$f_c(z) = \text{energy deposition efficiency per channel}$

(obtained using tabulated transfer fns $T^c(z, z', E)$ [Slatyer '15])

For 21 cm signal probes: Halo Contributions

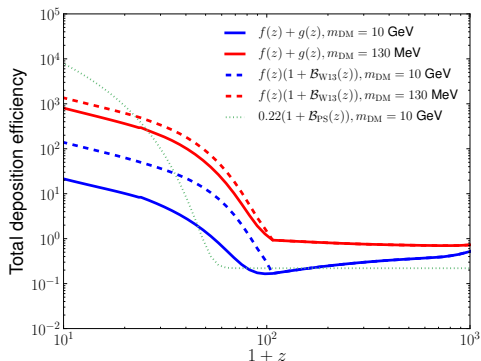
$$\left(\frac{dE(z)}{dt dV} \right)_{\text{injected}} = \frac{\langle \sigma v \rangle}{m_{\text{DM}}} n_{\text{DM}}^2(z) [1 + \mathcal{B}(z)]$$

$$\mathcal{B}(z) \propto \int_{M_{\text{min}}} \frac{dn(M, z)}{dM} dM \int_0^{R_{\text{vir}}} \rho^2(r) 4\pi r^2 dr$$

For 21 cm signal probes: Halo Contributions

$$\left(\frac{dE(z)}{dt dV} \right)_{\text{injected}} = \frac{\langle \sigma v \rangle}{m_{\text{DM}}} n_{\text{DM}}^2(z) [1 + \mathcal{B}(z)]$$

$$\mathcal{B}(z) \propto \int_{M_{\text{min}}} \frac{dn(M, z)}{dM} dM \int_0^{R_{\text{vir}}} \rho^2(r) 4\pi r^2 dr$$



$$\int dz' [1 + \mathcal{B}(z')] T^c(z, z', E)$$

$$\neq f_c(z) [1 + \mathcal{B}(z)]$$

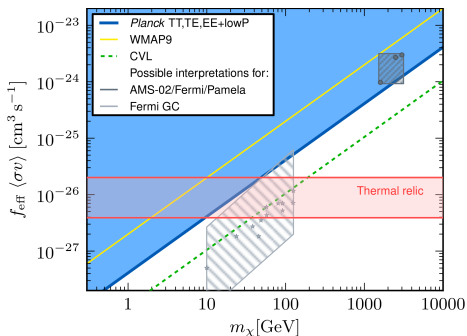
see e.g. [Slatyer'12]

$$\left(\frac{dE_c(z)}{dt dV} \right)_{\text{deposited}} \propto [f_c(z) + g_c(z)]$$

We use $M_{\text{min}} = 10^{-12} M_{\odot}$ and $10^{-6}, 10^{-3} M_{\odot}$ and take $dn(M, z)/dM$ from [Watson '13]

CMB constraints on DM annihilation: very Brief

see e.g. [Chen'03, Padmanabhan'05, Cirelli'09, Slatyer'09, Galli'11, Giesen'12, LLH'13, Galli'13, Madhavacheril'13, Poulin'15,...]



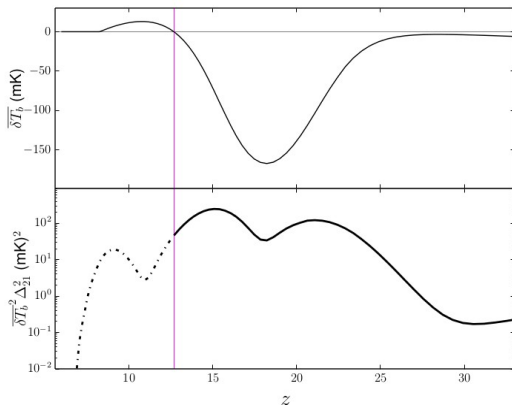
- This energy injections can **modify the history of recombination** and **affect CMB temperature and polarisation anisotropies**

m_{DM} [GeV]	0.001	0.009	0.13	1.1	10
$\langle\sigma v\rangle$ [cm ³ /s]	10^{-30}	10^{-29}	10^{-28}	10^{-27}	10^{-26}

- **Advantage** of CMB compared to other DM annihilation probes: **do not suffer astrophysics uncertainties** (such as ρ_{DM}) and **no contributions from halos** for σv independent of v (s-wave annihilation) [LLH'13, Poulin'15, Hongwan'16].

Impact of DM with s-wave annihilation

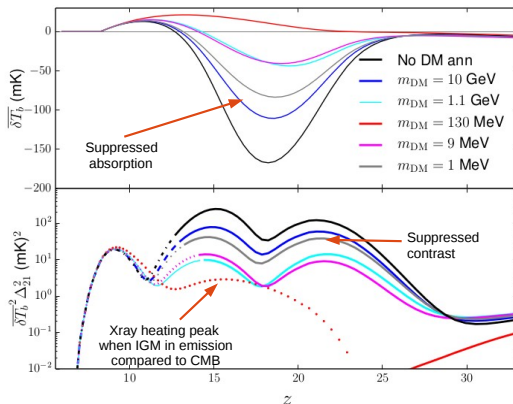
DM imprint \equiv earlier and uniform heating of the IGM, see also [Valdes'13, Evoli'14]



Obtained using 21cmFast code [Mesinger'10] modeling inhomogeneous ionization and heating and integrating the evolution of structures and radiation fields.

Impact of DM with s-wave annihilation

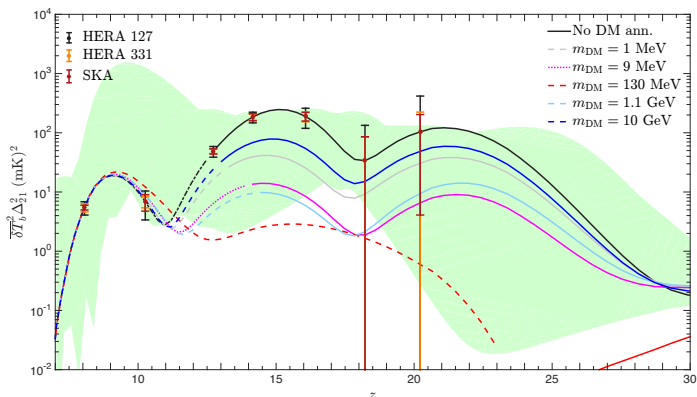
DM imprint \equiv earlier and uniform heating of the IGM, see also [Valdes'13, Evoli'14]



Obtained using 21cmFast code [Mesinger'10] modeling inhomogeneous ionization and heating and integrating the evolution of structures and radiation fields.

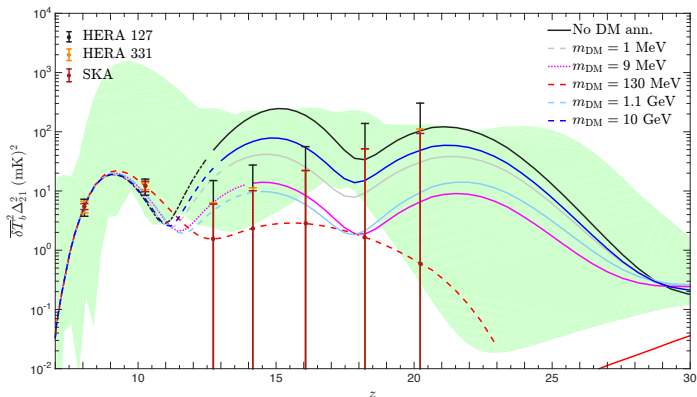
Theoretical uncertainties and experimental forecasts

- Large astro uncertainties (green region \equiv varying $N_\alpha, \zeta_X, dn/dM, M_{\text{vir}}$).
- Assuming complete foreground removal (using 21cmSense)
 - promising sensitivity for $z < 16$ for default model



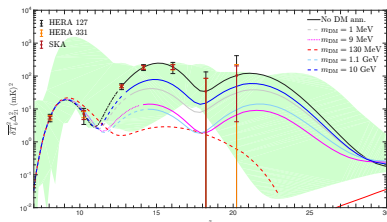
Theoretical uncertainties and experimental forecasts

- Large astro uncertainties (green region \equiv varying $N_\alpha, \zeta_X, dn/dM, M_{\text{vir}}$).
- Assuming complete foreground removal (using 21cmSense)
 - promising sensitivity for $z < 16$ for default model
 - DM with significant impact \rightsquigarrow suppressed signal \rightsquigarrow larger errors



Conclusion

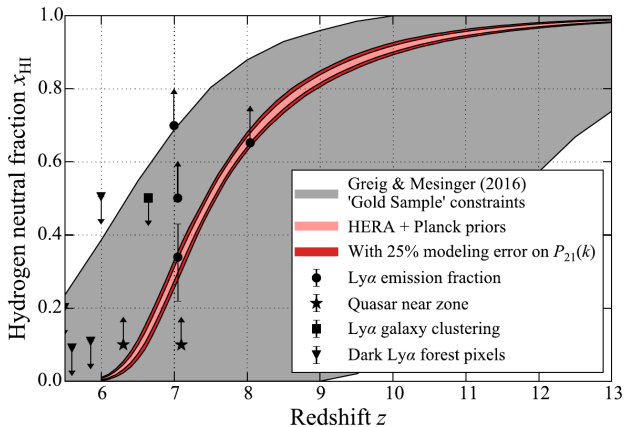
21cm signal \equiv unique window on EoR and dark ages



- DM can leave distinctive signatures on IGM at $10 < z < 30$ for $m_{DM} \sim 100$ MeV: strong suppression of the P_{21} at large z & X-ray peak in emission
- for other DM scenarios, disentangling DM imprint from astro is a challenging task
- Among the astro parameters the halo mass function $dn(z)/dM$ also drives the star formation rate \rightsquigarrow extra uncertainty on the 21cm signal

Thank you for your attention!

Backup

HERA reach on x_{HI} 

[De Boer'16]

Current constraints on EoR $\delta T_b^2 \Delta_{21}$

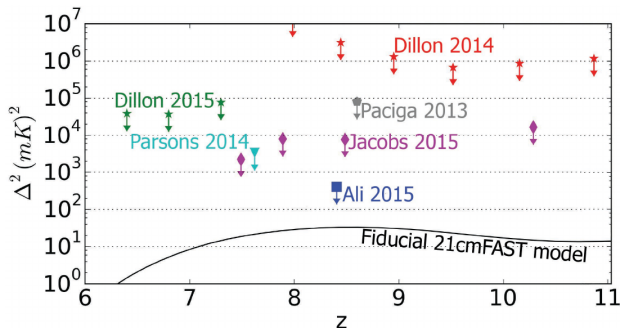


Figure 9. The current best published 2σ upper limits on the 21cm power spectrum, $\Delta^2(k)$, compared to a 21cmFAST-generated model at $k = 0.2 h \text{ Mpc}^{-1}$. Analysis is still underway on PAPER and MWA observations that approach their projected full sensitivities; HERA can deliver sub- mK^2 sensitivities.

[De Boer'16]

Current and future reach on $\delta T_b^2 \Delta_{21}$

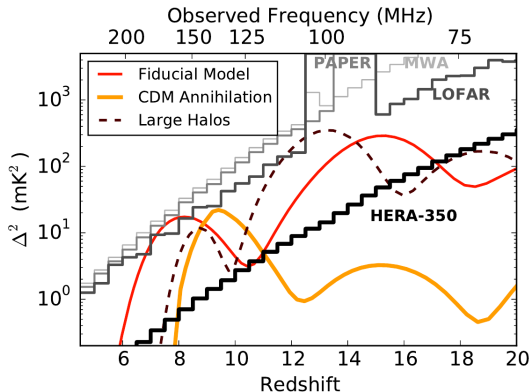


Figure 4. 1σ thermal noise errors on $\Delta^2(k)$, the 21 cm power spectrum, at $k=0.2 h \text{ Mpc}^{-1}$ (the dominant error at that k) with 1080 hours of integration (black) compared with various heating and reionization models (colored). Sensitiv-

[De Boer'16]

Resonant scattering of Ly α photons

Cause spin flip transitions

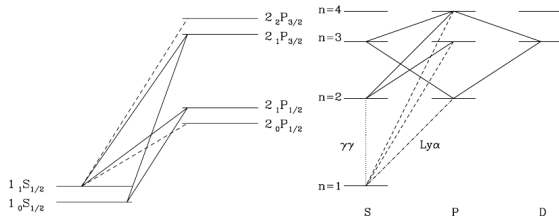


Figure 2. *Left panel:* Hyperfine structure of the hydrogen atom and the transitions relevant for the Wouthuysen-Field effect [24]. Solid line transitions allow spin flips, while dashed transitions are allowed but do not contribute to spin flips. *Right panel:* Illustration of how atomic cascades convert Ly n photons into Ly α photons.

[Pritchard'11]

Characterization of the 21cm signal

The observed brightness of a patch of HI relative to the CMB at $\nu = \nu_0/(1+z)$ is associated to the differential brightness temperature δT_b :

$$\delta T_b(\nu) \simeq 27 x_{\text{HI}} (1 + \delta_b) \left(1 - \frac{T_{\text{CMB}}}{T_S}\right) \left(\frac{1}{1 + H^{-1} \partial v_r / \partial r}\right) \left(\frac{1+z}{10}\right)^{1/2} \left(\frac{0.15}{\Omega_m h^2}\right)^{1/2} \left(\frac{\Omega_b h^2}{0.023}\right) \text{ mK}$$

Fraction of neutral H

Spin temperature= excitation T of 21cm line

T_S characterises the relative occupancy of the 2 HI ground state energy levels:
 $n_1/n_0 = 3 \exp[-h\nu_0/(k_B T_S)]$ and is driven by

Characterization of the 21cm signal

The **observed brightness of a patch of HI relative to the CMB at $\nu = \nu_0/(1+z)$** is associated to the differential brightness temperature δT_b :

$$\delta T_b(\nu) \simeq 27 x_{\text{HI}} (1 + \delta_b) \left(1 - \frac{T_{\text{CMB}}}{T_S}\right) \left(\frac{1}{1 + H^{-1} \partial v_r / \partial r}\right) \left(\frac{1+z}{10}\right)^{1/2} \left(\frac{0.15}{\Omega_m h^2}\right)^{1/2} \left(\frac{\Omega_b h^2}{0.023}\right) \text{ mK}$$

↑
↑
 Fraction of neutral H Spin temperature= excitation T of 21cm line

T_S characterises the relative occupancy of the 2 HI ground state energy levels:
 $n_1/n_0 = 3 \exp[-h\nu_0/(k_B T_S)]$ and is driven by

- **Scattering of CMB photons**

if CMB alone \rightsquigarrow **thermalisation $T_S = T_{\text{CMB}} \rightsquigarrow$ IGM unobservable**

Characterization of the 21cm signal

The **observed brightness of a patch of HI relative to the CMB** at $\nu = \nu_0/(1+z)$ is associated to the differential brightness temperature δT_b :

$$\delta T_b(\nu) \simeq 27 x_{\text{HI}} (1 + \delta_b) \left(1 - \frac{T_{\text{CMB}}}{T_S}\right) \left(\frac{1}{1 + H^{-1} \partial v_r / \partial r}\right) \left(\frac{1+z}{10}\right)^{1/2} \left(\frac{0.15}{\Omega_m h^2}\right)^{1/2} \left(\frac{\Omega_b h^2}{0.023}\right) \text{ mK}$$

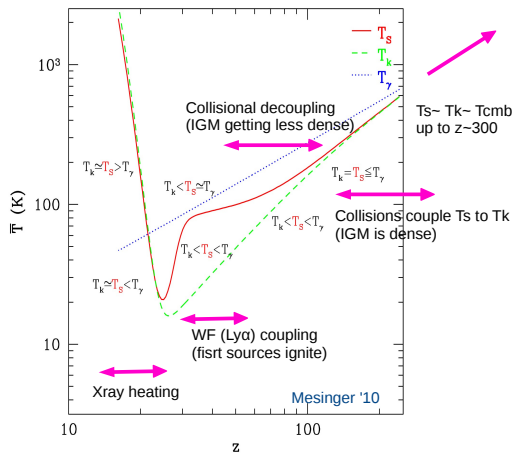
↑
↑
 Fraction of neutral H Spin temperature = excitation T of 21cm line

T_S characterises the relative occupancy of the 2 HI ground state energy levels:
 $n_1/n_0 = 3 \exp[-h\nu_0/(k_B T_S)]$ and is driven by

- **Scattering of CMB photons**
 if CMB alone \rightsquigarrow **thermalisation** $T_S = T_{\text{CMB}} \rightsquigarrow$ **IGM unobservable**
- **Atomic collisions** with H, p or e^- (when IGM is dense, dark ages)
- **Scattering of Ly α photons** \equiv Wouthuysen-Field (WF) effect
 (once early radiation sources light on)
 \rightsquigarrow **IGM is seen in absorption or emission** compared to CMB
 i.e. when $T_K \neq T_{\text{CMB}}$ and some mechanism couples T_K to T_S

Temperatures evolution

$$\delta T_b(\nu) \simeq 27 x_{\text{HI}} (1 + \delta_b) \left(1 - \frac{T_{\text{CMB}}}{T_S}\right) \left(\frac{1}{1 + H^{-1} \partial v_r / \partial r}\right) \left(\frac{1+z}{10}\right)^{1/2} \left(\frac{0.15}{\Omega_m h^2}\right)^{1/2} \left(\frac{\Omega_b h^2}{0.023}\right) \text{ mK}$$



From *injected* energy to *deposited*

see e.g. [Ripamonti'06, Slatyer'09, Valdes'10, Evoli'12, Slatyer'12, Galli'13, Weniger'13, **Slatyer'15**, Hongwan'16]

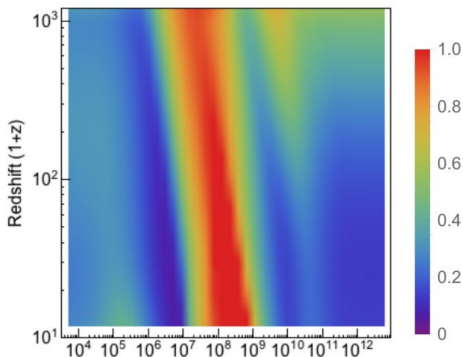
$$\epsilon_c^{\text{DM}}(\mathbf{x}, z) \equiv f_c(z) \left(\frac{dE_c(\mathbf{x}, z)}{dt dV} \right)_{\text{injected}}^{\text{smooth}}$$

$\sum_c f_c(z)$ for $\chi\chi \rightarrow e^+e^-$ [Slatyer'15]
as fn of E_{inj} of 1 member of e^+e^- pair and z_{abs}

$f_c(z)$ = energy deposition efficiency
per channel \equiv amount of energy
absorbed by the medium at z
including contributions from
particles injected at all $z' > z$

(obtained using tabulated transfer fns

$T^c(z, z', E)$ [Slatyer '15])



From *injected* energy to *deposited*

see e.g. [Ripamonti'06, Slatyer'09, Valdes'10, Evoli'12, Slatyer'12, Galli'13, Weniger'13, **Slatyer'15**, Hongwan'16]

$$\epsilon_c^{\text{DM}}(\mathbf{x}, z) \equiv f_c(z) \left(\frac{dE_c(\mathbf{x}, z)}{dtdV} \right)_{\text{injected}}^{\text{smooth}}$$

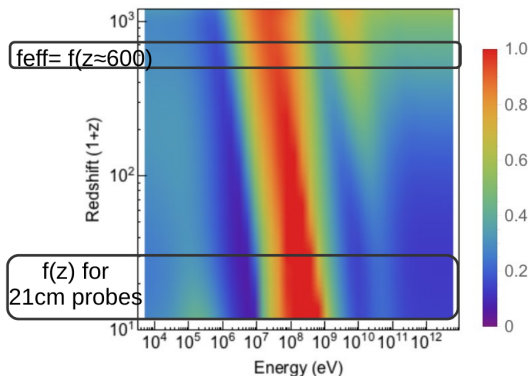
$\sum_c f_c(z)$ for $\chi\chi \rightarrow e^+e^-$ [Slatyer'15]
as fn of E_{inj} of 1 member of e^+e^- pair and z_{abs}

$f_c(z)$ = energy deposition efficiency

per channel \equiv amount of energy absorbed by the medium at z including contributions from particles injected at all $z' > z$

(obtained using tabulated transfer fns

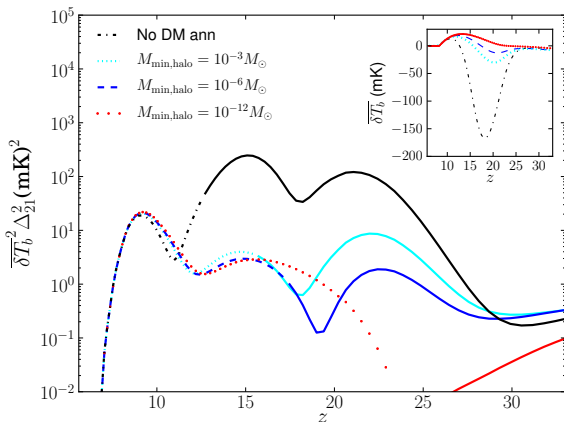
$T^c(z, z', E)$ [Slatyer '15])



Minimum Halo mass

$$\mathcal{B}(z) \propto \int_{M_{\min}} \frac{dn(M, z)}{dM} dM \int_0^{R_{\text{vir}}} \rho^2(r) 4\pi r^2 dr$$

Even for $M_{\min} = 10^{-3} M_{\odot}$
 \rightsquigarrow X-ray heating peak
 (partially) in emission for
 $m_{\text{DM}} = 130 \text{ MeV}$



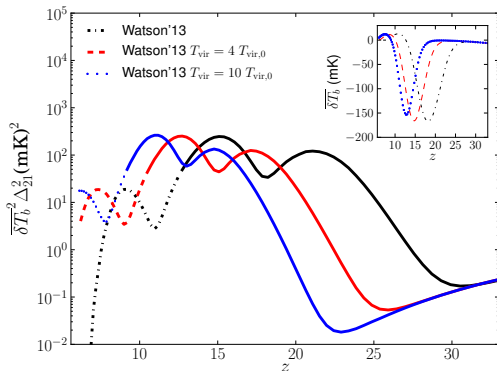
Minimum virial Temperature / Mass

$$f_{\text{coll}}(> M_{\text{vir}}) = \int_{M_{\text{vir}}} \frac{M}{\rho_0} \frac{dn(M, z)}{dM} dM,$$

Threshold for efficient star formation: $T_{\text{vir}} > T_{\text{vir},0} = 10^4 \text{ K}$

($\equiv M_{\text{vir},0}(z=10) = 3 \cdot 10^7 M_{\odot}$) [Evrard'90, Blanchard'92, Tegmark'96, Haiman'99, Ciardi'99]

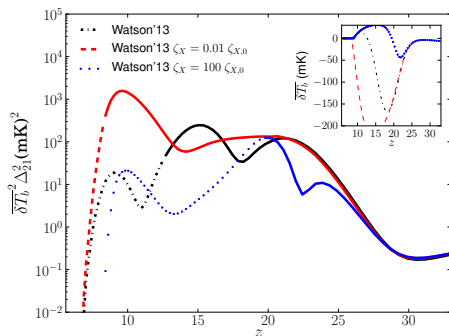
$$M_{\text{vir}} \simeq 10^8 \left(\frac{T_{\text{vir}}}{2 \cdot 10^4 \text{ K}} \frac{10}{1+z} \right)^{3/2} M_{\odot}$$



\rightsquigarrow larger M_{vir} threshold implies a delay in the X-ray and UV sources.

X-ray efficiency

X-ray emission rate is directly proportional to the number of X-ray photons per M_{\odot} in stars: ζ_X



$$\zeta_{X,0} = 10^{56} M_{\odot}^{-1} \leftrightarrow N_X \simeq 0.1$$

increasing ζ_X

\rightsquigarrow earlier X-ray heating

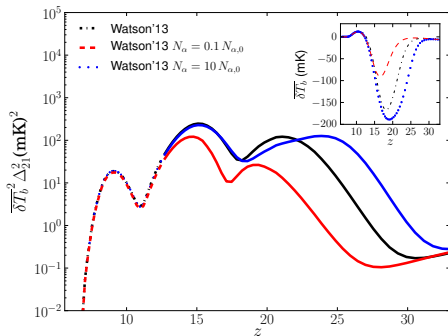
- less pronounced dip in $\delta \bar{T}_b$
- earlier X-ray peak in P_{21}

Ly_α contribution from stars

The direct stellar emission of photons between Ly_α and the Lyman limit will redshift until they enter a Lyman series resonance and subsequently, may generate Ly_α photons.

Increasing N_α
(driving $J_{\alpha,\star}$):

- deeper trough in $\delta\bar{T}_b$
- earlier Ly_α peak in P_{21}



$N_{\alpha,0}$ assumes Pop II stars [Barkana'04],

normalizing their emissivity to ~ 4400 ionizing photons per stellar baryon

Evolution equations

- Ionized fraction:

$$\frac{dx_e(\mathbf{x}, z)}{dz} = \frac{dt}{dz} (\Lambda_{\text{ion}} - \alpha_A C x_e^2 n_b f_H)$$

- Gas temperature:

$$\frac{dT_K(\mathbf{x}, z)}{dz} = \frac{2}{3 k_B (1 + x_e)} \frac{dt}{dz} \sum_{\beta} \epsilon_{\beta} + \frac{2 T_K}{3 n_b} \frac{dn_b}{dz} - \frac{T_K}{1 + x_e} \frac{dx_e}{dz},$$

- Ly α background:

$$J_{\alpha} = J_{\alpha, X} + J_{\alpha, \star} + J_{\alpha, \text{DM}}$$

Evolution equations

- Ionized fraction:

$$\frac{dx_e(\mathbf{x}, z)}{dz} = \frac{dt}{dz} (\Lambda_{\text{ion}} - \alpha_A C x_e^2 n_b f_H)$$

- Gas temperature:

$$\frac{dT_K(\mathbf{x}, z)}{dz} = \frac{2}{3 k_B (1 + x_e)} \frac{dt}{dz} \sum_{\beta} \epsilon_{\beta} + \frac{2 T_K}{3 n_b} \frac{dn_b}{dz} - \frac{T_K}{1 + x_e} \frac{dx_e}{dz},$$

- Ly α background:

$$J_{\alpha} = J_{\alpha, X} + J_{\alpha, * } + J_{\alpha, \text{DM}}$$

\rightsquigarrow we make use of 21cmFast to generate the 21cm background signal and powerspectrum.

DM contributions

- Ionized fraction and for the kinetic temperature of the gas

$$\Lambda_{\text{ion}}|_{\text{DM}} = f_{\text{H}} \frac{\epsilon_{\text{HI}}^{\text{DM}}}{E_{\text{HI}}} + f_{\text{He}} \frac{\epsilon_{\text{HeI}}^{\text{DM}}}{E_{\text{HeI}}}, \quad (1)$$

$$\left. \frac{dT_K}{dz} \right|_{\text{DM}} = \frac{dt}{dz} \frac{2}{3 k_B (1 + x_e)} \epsilon_{\text{heat}}^{\text{DM}}, \quad (2)$$

where $E_{\text{HI,HeI}}$ are the ionization energies for hydrogen and helium and $f_{\text{He}} = N_{\text{He}}/N_b$ is the helium number fraction.

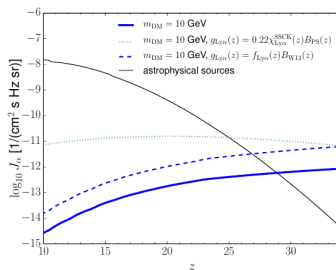
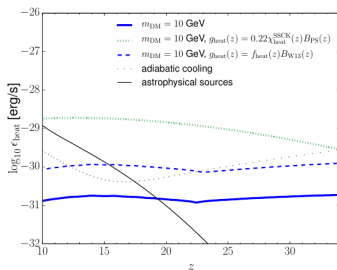
- The Ly α flux

$$J_{\alpha, \text{DM}} = \frac{c n_b \epsilon_{\text{Ly}\alpha}^{\text{DM}}}{4\pi h\nu_{\alpha}} \frac{1}{H(z)\nu_{\alpha}}, \quad (3)$$

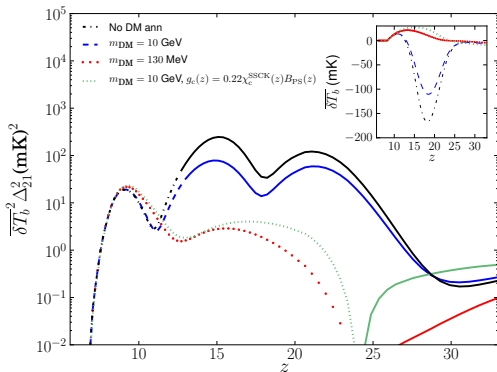
where ν_{α} is the emission frequency of a Ly α photon.

Previous analysis

Comparison with a reproduction of DM energy deposition rate corresponding to annihilations into $\mu^+\mu^-$ considering PS formalism from [Evoli'14],



Previous analysis : comparison



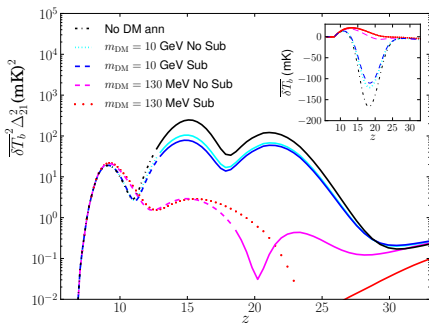
- *The X-ray heating peak could occur when the IGM is already in emission against the CMB: we only do reach that conclusion for the most extreme of our cases, $m_{DM} = 130$ MeV, $\langle\sigma v\rangle = 10^{-28}$ cm³/s and $M_{\min} = 10^{-12} M_{\odot}$.*

- *With DM annihilations the X-ray heating peak in the 21 cm power could be lower than the other two peaks: not for the case considered in [Evoli'14] but ok for $m_{DM} = 130$ MeV and $\langle\sigma v\rangle = 10^{-28}$ cm³/s, even for $M_{\min} = 10^{-3} M_{\odot}$.*
- *Dramatic drop in large-scale power between the Ly α pumping and X-ray heating epochs. This feature is only seen for the most extreme case we consider.*

For 21 cm signal probes: Halo Contributions- Substructures

$$\int_0^{R_{\text{vir}}} \rho^2(r) 4\pi r^2 dr$$

$$\rightarrow \int_0^{R_{\text{vir}}} \rho^2(r) 4\pi r^2 dr + \int_{M_{\text{min}}}^M \frac{dn_{\text{sub}}}{dm} dm \int_0^{r_{\text{vir}}} \rho_{\text{sub}}^2(r_{\text{sub}}) 4\pi r_{\text{sub}}^2 dr_{\text{sub}} ,$$



dn_{sub}/dm is the comoving subhalo mass function, m is the subhalo mass, $\rho_{\text{sub}}(r_{\text{sub}})$ is the subhalo density profile, and r_{vir} is the subhalo virial radius. For the subhalo mass function in a host halo of mass M , we use

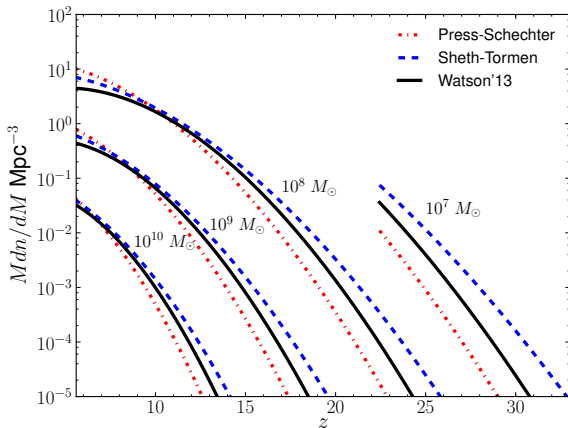
$$dn_{\text{sub}}/dm = A/M (m/M)^{-\alpha},$$

(α in the range [1.9, 2] in simu [Diemand:2006ik, Madau:2008fr, Springel:2008cc]). We took $\alpha = 2$ and we set $A = 0.012$ [Sanchez-Conde:2013]

Halo mass function

Ionization, heating and excitation critically depend on the fraction of mass collapsed in halos

$$f_{\text{coll}}(> M_{\text{vir}}) = \int_{M_{\text{vir}}} \frac{M}{\rho_0} \frac{dn(M, z)}{dM} dM,$$



Halo contribution from N-body simulations

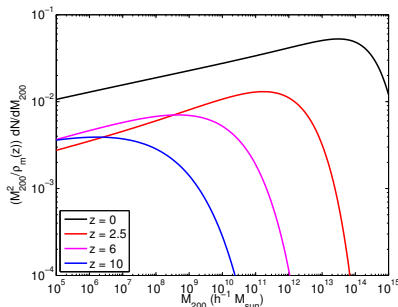
$$G(z) \equiv \frac{1}{(\Omega_{\text{DM},0} \rho_{c,0})^2} \frac{1}{(1+z)^6} \int_{M_{\text{min}}}^{\infty} dM \frac{dn(M,z)}{dM} \int_0^{r_{\Delta}} dr 4\pi r^2 \rho_{\text{halo}}^2(r) .$$

- For NFW profile:

$$\int_0^{r_{\Delta}} dr 4\pi r^2 \rho_{\text{halo}}^2(r) = \tilde{g}(c_{\Delta}) \frac{M \Delta \rho_c(z)}{3}$$

The concentration param. c_{Δ} is obtained from MultiDark/BigBolshoi simulations [Prada '11] (the fitting function is extrapolated outside limited simul. range)

- $\frac{dn_{\text{halo}}(M,z)}{dM} = \frac{\rho_m(z)}{M^2} \frac{d \ln \sigma^{-1}}{d \ln M} f(\sigma, z) ,$



The parametrization of the differential mass function $f(\sigma, z)$ is based on the results obtained in [Watson'12] by using the CubeP³M halofinder (CPMSO) and the Amiga Halo Finder (AHF). We have used this fit outside the range where it was obtained, $-0.55 \leq \ln \sigma^{-1} \leq 1.35$, with $\sigma(M, z)$ the rms density fluctuation, across all redshifts There could be differences of up to a few orders of magnitude with respect to other parametrizations.

HI 21 cm line – δT_b

$$y_\alpha = \frac{P_{10} T_*}{A_{10} T_k}$$

$$y_c = \frac{C_{10} T_*}{A_{10} T_k}$$

- A_{10} : spontaneous decay rate of the hyperfine transition of hydrogen
- P_{10} : indirect de-excitation rate of the triplet via absorption of a Ly α photon = 4/27 the rate at which Ly α photons are scattered by HI
- C_{10} : collisional de-excitation rate

Once T_s has been determined we can obtain the 21 cm radiation intensity which can be expressed by the differential brightness temperature between a neutral hydrogen patch and the CMB:

$$\delta T_b \simeq \frac{T_S - T_{CMB}}{1 + z} \tau$$

$$\tau \simeq \frac{3c^3 h_p A_{10}}{32\pi k_B \nu_0^2 T_S H(z)} \mathcal{N}_{HI}$$



Spin Temperature

HI 21 cm line

HI 21 cm tomography: a powerful tool for future observations

Emission/absorption of 21cm photons governed by the HI spin temperature T_s

$$\frac{n_1}{n_0} = 3 \exp\left(-\frac{T_\star}{T_s}\right)$$

CMB radiation forces $T_s \sim T_{\text{CMB}}$ on a short timescale ($\sim 10^4$ yr).

HI will not emit nor absorb

Two mechanisms can decouple T_s from T_{CMB} :

- Collisions (effective at $z > 70$ due to the higher mean gas density)
- Scattering by Ly α photons , Wouthuysen-Field (WF) process

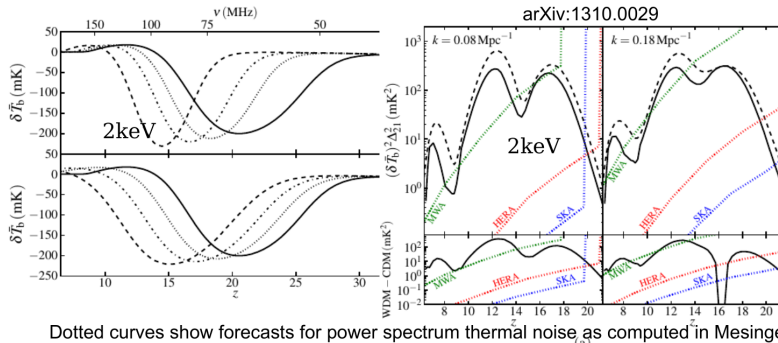
$$T_s = \frac{T_{\text{CMB}} + y_\alpha T_k + y_c T_k}{1 + y_\alpha + y_c}$$



WDM beyond EOR

mDM \sim keV \rightarrow increased particle free-streaming and velocity dispersion
 \rightarrow suppress structures on small-scales.

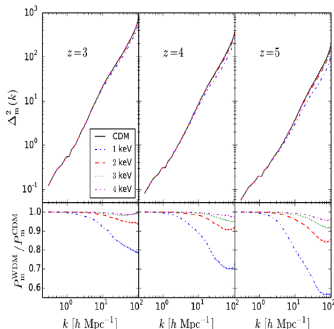
- The resulting dearth of galaxies in the early Universe means that the **astrophysical epochs in the 21cm signal were delayed**.
- The galaxies driving the 21cm evolution in WDM should reside in higher mass, more rapidly evolving halos, than those in CDM. The **increased bias of such halos results in a larger 21cm fluctuations**



Dotted curves show forecasts for power spectrum thermal noise as computed in Mesinger et al. 2013a with 2000h time.

WDM at low redshifts

Analyse 21cm intensity mapping in the post-reionization Universe at $z = 3 - 5$ with hydrodynamical simulations for 5 different models: cold dark matter and WDM with 1,2,3,4 keV



arXiv:1502.06961

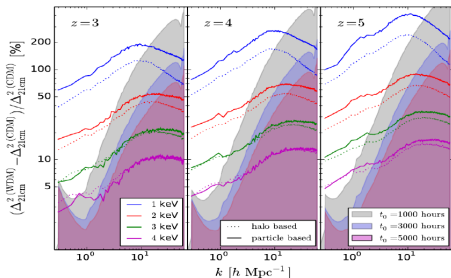


Figure 11. Relative difference between the 21cm power spectrum of the models with WDM and CDM where the HI distribution is modeled using the halo based method (dotted lines) and the particle based method (solid lines). Results are shown at $z = 3$ (left), $z = 4$ (middle) and $z = 5$ (right). The error on the 21cm power spectrum of the model with CDM, normalized to the amplitude of the 21cm power spectrum: $\sigma_{\Delta_{21\text{cm}}^2} / \Delta_{21\text{cm}}^2$, is shown in a shaded region for three different observation times: $t_0 = 1000$ hour (grey), $t_0 = 3000$ hours (blue) and $t_0 = 5000$ hours (purple). For clarity, we show the error on $\Delta_{21\text{cm}}^2$ from one HI-assignment method only because both are very similar and overlap at the scale of the plot.

5000 hours of observations \rightarrow 4 keV WDM model can be ruled out at more than 1σ at $z = 3$ and at more than 2σ at $z = 5$ (make use only of the largest scales $k < 1 - 3$ h Mpc $^{-1}$ available, since the small scale signal is hindered by noise (see figure 11))

In practice how to proceed

- What does DM annihilate into?:
 - neutrinos \rightsquigarrow escape constraints from CMB
 - $f\bar{f}, \gamma, W^+W^-, \dots \rightsquigarrow e^+, e^-, \gamma$ using e.g. [Pythia, Mardon'09, PPPC4DMID]

In practice how to proceed

- What does DM annihilate into?:
 - neutrinos \rightsquigarrow escape constraints from CMB
 - $f\bar{f}, \gamma, W^+W^-, \dots \rightsquigarrow e^+, e^-, \gamma$ using e.g. [Pythia, Mardon'09, PPPC4DMID]
- Rate of heating or ionization depends on see e.g. [Chen'03, Padmanabhan'05, Galli'13]
 $\chi_i(z)$ = fraction of injected energy into i = heat, ionization, excitation

$$\mathcal{F}(z) = \frac{\chi_i(z)}{H(z)(1+z)n_H(z)} \left(\frac{dE}{dt dV} \right)_{\text{deposit}}$$

In practice how to proceed

- **What does DM annihilate into?:**
 - neutrinos \rightsquigarrow escape constraints from CMB
 - $f\bar{f}, \gamma, W^+W^-, \dots \rightsquigarrow e^+, e^-, \gamma$ using e.g. [Pythia, Mardon'09, PPPC4DMID]
- **Rate of heating or ionization depends on** see e.g. [Chen'03, Padmanabhan'05, Galli'13]
 $\chi_i(z)$ = fraction of injected energy into i = heat, ionization, excitation

$$\mathcal{F}(z) = \frac{\chi_i(z)}{H(z)(1+z)n_H(z)} \left(\frac{dE}{dt dV} \right)_{\text{deposit}} \propto \chi_i(z) \times f(z) \times \begin{cases} (1+z)^{1/2} & \text{s-wave ann} \\ (1+z)^{-5/2} & \text{decay} \end{cases}$$

$$\left(\frac{dE}{dt dV} \right)_{\text{deposit}} = f(z) \left(\frac{dE}{dt dV} \right)_{\text{inject}} \propto f(z) \times \begin{cases} n_{DM}^2 \langle \sigma v \rangle & \text{annihil} \\ n_{DM} / \tau_{DM} e^{-t/\tau_{DM}} & \text{decay} \end{cases}$$

s-wave annihilating dark matter Modify the Recombination History

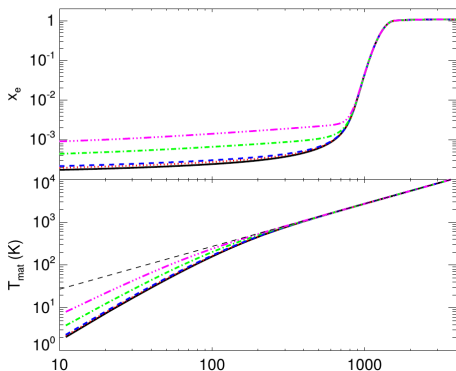
$$\left(\frac{dE}{dt dV} \right)_{\text{deposit}} \propto f(z) n_{DM}^2 \langle \sigma v \rangle$$

$$\langle \sigma v \rangle \propto a = cst$$

$$\mathcal{F}(z) \propto (1+z)^{1/2}$$

“early time effect”

Recombination history and power spectra modified

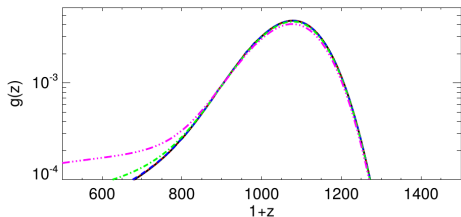


- increased residual ionization
- increased IGM temperature

$$f(z) \langle \sigma v \rangle \sim 10^{-27}, 2 \cdot 10^{-27}, 2 \cdot 10^{-26}, 10^{-25} \text{ cm}^3/\text{s}$$

for $m_{DM} = 1 \text{ GeV}$ [Padmanabhan'05]

Recombination history and power spectra modified



$f(z)\langle\sigma v\rangle \sim 10^{-27}, 2 \cdot 10^{-27}, 2 \cdot 10^{-26}, 10^{-25} \text{ cm}^3/\text{s}$
 for $m_{DM} = 1 \text{ GeV}$ [Padmanabhan'05]

- increased residual ionization
- increased IGM temperature
- affects the optical depth τ to recombination with:

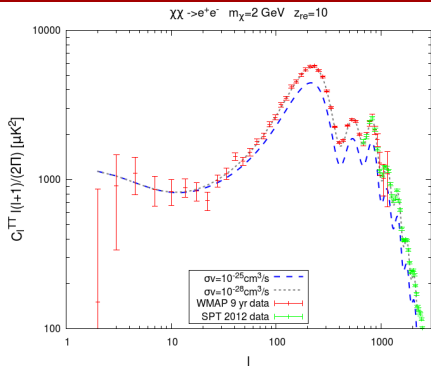
$$\dot{\tau} = -\sigma_T x_e n_b a$$

and the visibility function

$$g(z) = -\dot{\tau} \exp(-\tau(z))$$

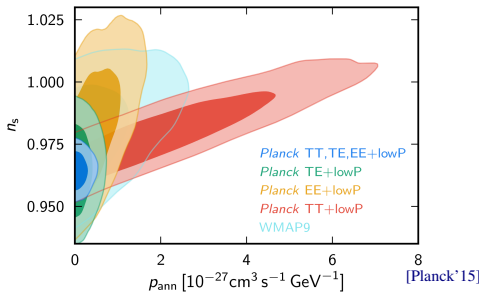
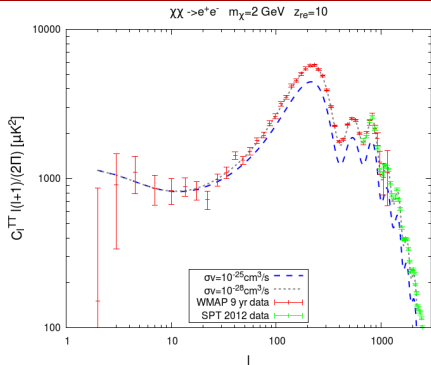
\equiv probability that a γ last scattered at z , very peaked around $z \sim 1000$

\rightsquigarrow broadening of the last scattering surface



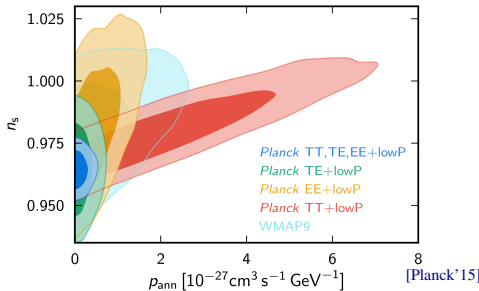
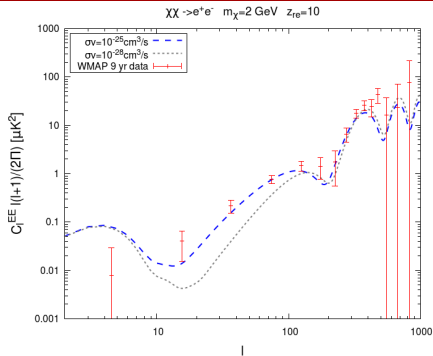
broadening of the last scattering surface :

- **attenuates of correlations** at small scales (large l) [Padmanabhan'05].



broadening of the last scattering surface :

- **attenuates of correlations** at small scales (large l) [Padmanabhan'05].
- The effect of annihilation $p_{\text{ann}} = f(z)\langle\sigma v\rangle/m_{DM}$ is **degenerate** with A_s , and n_s driving the amplitude of the C_l [Padmanabhan'05, Madhavacheril'13, Planck'15].



broadening of the last scattering surface :

- **attenuates of correlations** at small scales (large l) [Padmanabhan'05].
- The effect of annihilation $p_{\text{ann}} = f(z)\langle\sigma v\rangle/m_{\text{DM}}$ is **degenerate with A_s , and n_s** driving the amplitude of the C_l [Padmanabhan'05, Madhavacheril'13, Planck'15].
- **increases the polarisation fluctuations** and shift the EE (TE) peaks at large scale [Padmanabhan'05].
- **Planck low l TE,EE spectra \rightsquigarrow break degeneracies and improve constraints** (by \sim one order of magnitude [Planck '15]).

p-wave annihilating dark matter

Late time energy injection

$$\left(\frac{dE}{dt dV} \right)_{\text{deposit}} \propto f(z) n_{DM}^2 \langle \sigma v \rangle$$

$$\langle \sigma v \rangle \propto bv^2 \quad \text{or} \quad \sigma v_{ref} \langle v \rangle^2 / v_{ref}^2$$

$$\mathcal{F}(z) \propto (1+z)^{1/2} \frac{(1+z)^2}{(1+z_{KD})^2} \quad \text{with} \quad z_{KD} \gg z_{rec}$$

Main constraints from DM halos: late time effect

Annihilation & Structure Formation

DM collapsing into structures will boost the annihilation rate, in the on the spot approximation see also [Natarajan '08+, Belikov '09, Cirelli'09, Kanzaki'09, Hustsi'11, Giesen'12]:

$$\left(\frac{dE}{dVdt} \right)_{\text{halo,injected}} = \frac{\langle \sigma v \rangle}{m_\chi} \rho_{DM,0}^2 (1+z)^6 (\mathbf{Bgd}(z) + \mathbf{Halo}(z))$$

Annihilation & Structure Formation

DM collapsing into structures will boost the annihilation rate, in the on the spot approximation see also [Natarajan '08+, Belikov '09, Cirelli'09, Kanzaki'09, Hustsi'11, Giesen'12]:

$$\left(\frac{dE}{dVdt} \right)_{\text{halo,injected}} = \frac{\langle \sigma v \rangle}{m_\chi} \rho_{DM,0}^2 (1+z)^6 (\text{Bgd}(z) + \text{Halo}(z))$$

Here we consider both s- and p-wave driven $\langle \sigma v \rangle$:

- **Smooth Contribution Bgd(z)**
supressed for p-wave annihilation

Annihilation & Structure Formation

DM collapsing into structures will boost the annihilation rate, in the on the spot approximation see also [Natarajan '08+, Belikov '09, Cirelli'09, Kanzaki'09, Hustsi'11, Giesen'12]:

$$\left(\frac{dE}{dVdt} \right)_{\text{halo, injected}} = \frac{\langle \sigma v \rangle}{m_\chi} \rho_{DM,0}^2 (1+z)^6 (\text{Bgd}(z) + \text{Halo}(z))$$

Here we consider both s- and p-wave driven $\langle \sigma v \rangle$:

- Smooth Contribution Bgd(z)
supressed for p-wave annihilation
- Structures Contribution Halo(z)

$$\text{Halo}(z) \propto \int_{M_{\min}}^{\infty} dM \frac{dn(M,z)}{dM} \int_0^{r_\Delta} dr 4\pi r^2 \rho_{\text{halo}}^2 \times \begin{cases} 1 & \text{s - wave} \\ \frac{\langle v^2 \rangle}{v_{\text{ref}}^2} & \text{p - wave} \end{cases}$$

We made use of [Multidark/BigBolshoi simulation](#) for the halo mass function $\frac{dn(M,z)}{dM}$ and NFW for ρ_{halo}

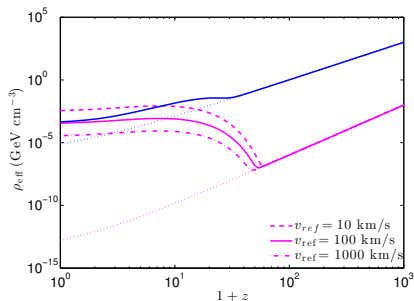
CMB sensitivity to annihilation + structure formation

In our full analysis, we took into account the energy deposition efficiency ($\equiv f(z)$ in s-wave Bgd case) using [Slatyer'12]:

- s-wave $\langle\sigma v\rangle = \text{cst}$

Despite enhancements of several orders of magnitude, **Halo(z)** contrib. is subdominant to early time ($z \sim z_{\text{rec}}$) energy injection.

Effective DM density



$$\rho_{\text{eff}} = \rho_{\text{DM},0}(1+z)^3 \sqrt{\text{Bgd}(z) + \text{Halo}(z)}$$

(on the spot approx. for plot)

CMB sensitivity to annihilation + structure formation

In our full analysis, we took into account the energy deposition efficiency ($\equiv f(z)$ in s-wave Bgd case) using [Slatyer'12]:

- s-wave $\langle\sigma v\rangle = \text{cst}$

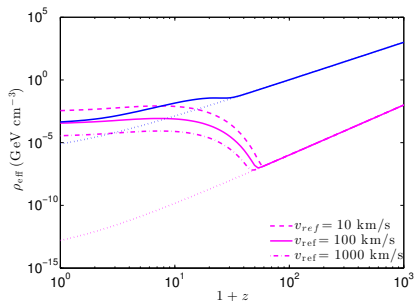
Despite enhancements of several orders of magnitude, Halo(z) contrib. is subdominant to early time ($z \sim z_{\text{rec}}$) energy injection.

- p-wave $\langle\sigma v\rangle = \sigma v_{\text{ref}} \langle v^2 \rangle / v_{\text{ref}}^2$

Bgd(z) severe suppression at early time by $\langle v^2 \rangle / v_{\text{ref}}^2$

\rightsquigarrow Halo (z) dominates energy deposition by orders of magnitude

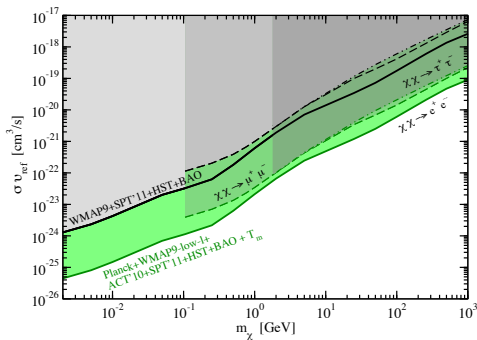
Effective DM density



$$\rho_{\text{eff}} = \rho_{\text{DM},0} (1+z)^3 \sqrt{\text{Bgd}(z) + \text{Halo}(z)}$$

(on the spot approx. for plot)

Constraints on p-wave annihilation



for $v_{ref} = 100 \text{ km/s}$

- Principal source of improvement between black and green lines: T_m constraints
- CMB constraints well above p-wave $\langle \sigma v \rangle$ for freeze-out
 \rightsquigarrow specifically relevant for other production mechanisms

Decaying dark matter

Late time energy injection

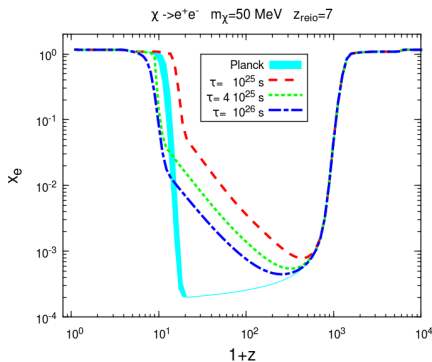
$$\left(\frac{dE}{dt dV} \right)_{\text{deposit}} \propto f(z) n_{DM} / \tau_{DM}$$

$$\mathcal{F}(z) \propto (1+z)^{-5/2}$$

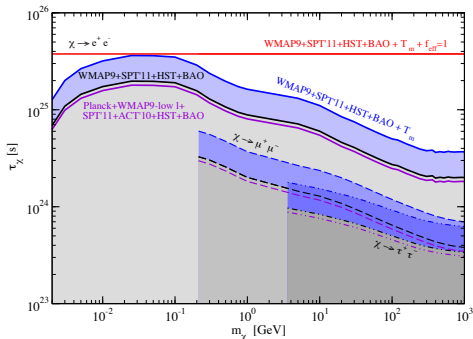
“late time effect”

DM decay

see also [Chen'03, Mapelli'06, Ripamonti'06, Zhang'07, Finkbeiner'11, Slatyer'12, Cline'13,...]



Late time energy injection
due to $\mathcal{F}(z) \propto (1+z)^{-5/2}$



Prior on IGM temperature $T_m \sim 10^4 K$
for $2 < z < 4.5$

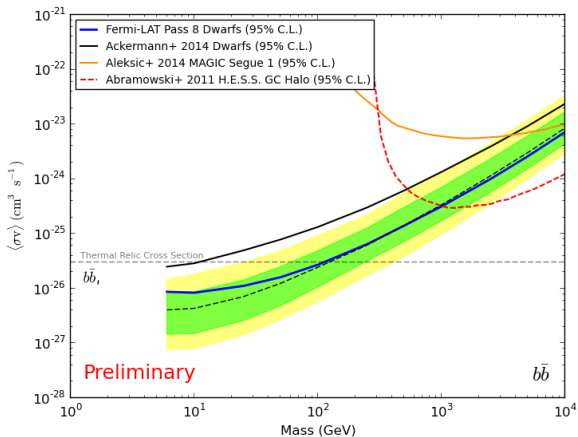
\rightsquigarrow lower bound on the DM lifetime,

$$\tau_\chi / f_{\text{eff,dec}}(m_\chi) \gtrsim 4 \times 10^{25} \text{ s.}$$

Fermi most recent (preliminary) results



Comparative Limits

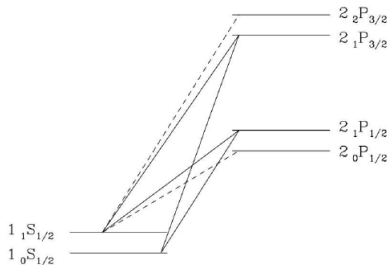


HI 21 cm line – WF process

F = total angular momentum of the atom

$\Delta F = 0, \pm 1 \setminus 0 \rightarrow 0$
(electric dipole selection rules)

An H atom in the singlet ground level that absorbs a Ly α photon and jumps to the 2p state is allowed to re-emit the Ly α photon and end up in the triplet ground level



In practice how to proceed

- What does DM annihilate into?:
 - neutrinos \rightsquigarrow escape constraints from CMB
 - $f\bar{f}, \gamma, W^+W^-, \dots \rightsquigarrow e^+, e^-, \gamma$ using e.g. [Pythia, Mardon'09, PPPC4DMID]

In practice how to proceed

- What does DM annihilate into?:
 - neutrinos \rightsquigarrow escape constraints from CMB
 - $f\bar{f}, \gamma, W^+W^-, \dots \rightsquigarrow e^+, e^-, \gamma$ using e.g. [Pythia, Mardon'09, PPPC4DMID]
- Rate of heating or ionization depends on see e.g. [Chen'03, Padmanabhan'05, Galli'13]

$$\mathcal{F}(z) = \frac{\chi_i(z)}{H(z)(1+z)n_H(z)} \left(\frac{dE}{dt dV} \right)_{\text{deposit}}$$

$\chi_i(z)$ = fraction of injected energy into i = heat, ionization, excitation

In practice how to proceed

- What does DM annihilate into?:
 - neutrinos \rightsquigarrow escape constraints from CMB
 - $f\bar{f}, \gamma, W^+W^-, \dots \rightsquigarrow e^+, e^-, \gamma$ using e.g. [Pythia, Mardon'09, PPPC4DMID]
- Rate of heating or ionization depends on see e.g. [Chen'03, Padmanabhan'05, Galli'13]

$$\mathcal{F}(z) = \frac{\chi_i(z)}{H(z)(1+z)n_H(z)} \left(\frac{dE}{dtdV} \right)_{deposit}$$

$\chi_i(z)$ = fraction of injected energy into i = heat, ionization, excitation

- From *injected* energy to *deposited*

see e.g. [Ripamonti'06, Slatyer'09, Valdes'10, Evoli'12, Slatyer'12, Galli'13, Weniger'13]

$$\left(\frac{dE}{dtdV} \right)_{deposit} = f(z) \left(\frac{dE}{dtdV} \right)_{inject} \propto f(z) \times \begin{cases} n_{DM}^2 \langle \sigma v \rangle & \text{annihil} \\ n_{DM} / \tau_{DM} e^{-t/\tau_{DM}} & \text{decay} \end{cases}$$

$f(z)$ = energy deposition efficiency: amount of energy absorbed by the medium at z including contributions from particles injected at all $z' > z$.

In practice how to proceed

- What does DM annihilate into?:
 - neutrinos \rightsquigarrow escape constraints from CMB
 - $f\bar{f}, \gamma, W^+W^-, \dots \rightsquigarrow e^+, e^-, \gamma$ using e.g. [Pythia, Mardon'09, PPPC4DMID]
- Rate of heating or ionization depends on see e.g. [Chen'03, Padmanabhan'05, Galli'13]

$$\mathcal{F}(z) = \frac{\chi_i(z)}{H(z)(1+z)n_H(z)} \left(\frac{dE}{dtdV} \right)_{deposit} \propto \chi_i(z) \times \begin{cases} (1+z)^{1/2} & \text{s-wave ann} \\ (1+z)^{-5/2} & \text{decay} \end{cases}$$

$\chi_i(z)$ = fraction of injected energy into i = heat, ionization, excitation

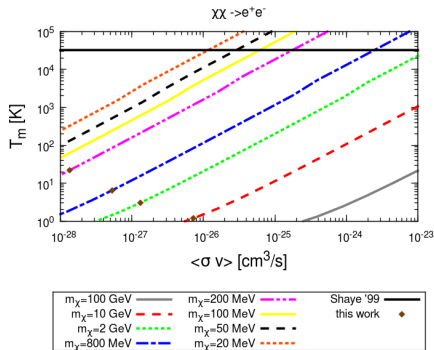
- From *injected* energy to *deposited*
see e.g. [Ripamonti'06, Slatyer'09, Valdes'10, Evoli'12, Slatyer'12, Galli'13, Weniger'13]

$$\left(\frac{dE}{dtdV} \right)_{deposit} = f(z) \left(\frac{dE}{dtdV} \right)_{inject} \propto f(z) \times \begin{cases} n_{DM}^2 \langle \sigma v \rangle & \text{annihil} \\ n_{DM} / \tau_{DM} e^{-t/\tau_{DM}} & \text{decay} \end{cases}$$

$f(z)$ = energy deposition efficiency: amount of energy absorbed by the medium at z including contributions from particles injected at all $z' > z$.

IGM temperature

IGM temperature can be considered as **extra constraint** see also [Cirelli'09, Giesen'12]:
 Ly- α observations at $2 < z < 4.5$ [Schaye] indicate that $T_m \sim 10^4$ K



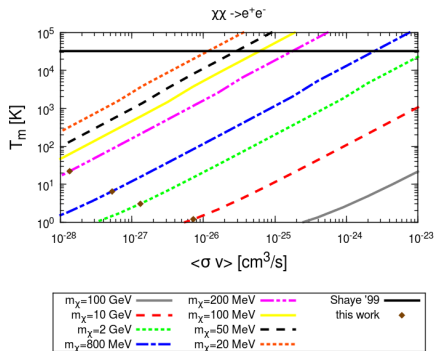
IGM temperature at $z = 3$
 for s-wave annihilation

- s-wave

$\langle \sigma v \rangle$ saturating T_m bound are
 orders of magnitude above CMB
 constraints

IGM temperature

IGM temperature can be considered as **extra constraint** see also [Cirelli'09, Giesen'12]:
 Ly- α observations at $2 < z < 4.5$ [Schaye] indicate that $T_m \sim 10^4$ K



IGM temperature at $z = 3$
 for s-wave annihilation

- s-wave

$\langle\sigma v\rangle$ saturating T_m bound are orders of magnitude above CMB constraints

- p-wave

T_m provide a **powerfull tool to constrain late time energy injection**

Priors

Parameter	Prior
$\Omega_{b,0}h^2$	$0.005 \rightarrow 0.1$
$\Omega_{\text{DM},0}h^2$	$0.01 \rightarrow 0.99$
Θ_s	$0.5 \rightarrow 10$
z_{reio}	$6 \rightarrow 12$
n_s	$0.5 \rightarrow 1.5$
$\ln(10^{10} A_s)$	$2.7 \rightarrow 4$
$\langle\sigma v\rangle/(3 \cdot 10^{-26} \text{cm}^3/\text{s})$	$10^{-5} \rightarrow 10^{2.5}$

Parameter	Prior
$\Omega_{b,0}h^2$	$0.005 \rightarrow 0.1$
$\Omega_{\text{DM},0}h^2$	$0.01 \rightarrow 0.99$
Θ_s	$0.5 \rightarrow 10$
z_{reio}	$7 \rightarrow 12$
n_s	$0.5 \rightarrow 1.5$
$\ln(10^{10} A_s)$	$2.7 \rightarrow 4$
$\tau_X/(10^{24} \text{s})$	$10^{-2} \rightarrow 10^5$
$\sigma v_{\text{ref}}/(3 \times 10^{-26} \text{cm}^3/\text{s})$	$10^0 \rightarrow 10^{12}$

f(z)

- High energy photons (GeV, TeV) or electrons do not deposit directly their energy in the medium.
- Their energy is degraded to ~ 3 keV [Slatyer'13] energy before being possibly absorbed by atomic processes (heat, ionisation, excitation)
- For high energy e^- the main energy loss is Inverse Compton Scattering (ICS) on the CMB $\gamma e \rightarrow \gamma e \rightsquigarrow$ effective injected photon spectrum
- For high energy γ we have (per order of increasing E)
 - photoionization
 - Compton scattering
 - pair production off nuclei: $\gamma A \rightarrow Ae\bar{e}$
 - photon photon scattering
- Photons produced originally or in the cooling cascade can fall into the “transparency window” depending on their energy (typically between 10^6 and 10^{12} eV) or redshift (at low redshift universe more transparent) \rightsquigarrow their energy is possibly never degraded to the atomic scale \rightsquigarrow part of diffuse γ background

Energy deposition s-wave

$$\left(\frac{dE}{dt dV} \right)_{\text{deposited}} = [f(z, m_\chi) + g(z, m_\chi)] (1+z)^6 (\Omega_{\text{DM},0} \rho_{c,0})^2 \zeta \frac{\langle \sigma v \rangle}{m_\chi},$$

- Bgd(z)

$$f(z, m_\chi) = \frac{H(z)}{(1+z)^3} \sum_i \int dE E \frac{dN_i(E, m_\chi)}{dE} \sum_i \int dz' \frac{(1+z')^2}{H(z')} \int dE T_i(z', z, E) E \frac{dN(E, m_\chi)}{dE}.$$

- Halo(z)

$$g(z, m_\chi) = \frac{H(z)}{(1+z)^3} \sum_i \int dE E \frac{dN}{dE} \sum_i \int dz' \frac{(1+z')^2}{H(z')} G(z') \int T_i(z', z, E) E \frac{dN}{dE} dE,$$

$$G(z) \equiv \frac{1}{(\Omega_{\text{DM},0} \rho_{c,0})^2} \frac{1}{(1+z)^6} \int_{M_{\text{min}}}^{\infty} dM \frac{dn(M, z)}{dM} \int_0^{r_\Delta} dr 4\pi r^2 \rho_{\text{halo}}^2(r).$$

- The factors of $(1+z')$ in the integral: $n_{\text{DM}}^2 \propto (1+z')^6$ & $dV \propto (1+z')^{-3}$ & $dt = -d \ln(1+z')/H(z')$

- M_{min} is very model dependent quantity that can vary from $M_{\text{min}} = 10^{-4} M_\odot$ to $M_{\text{min}} = 10^{-11} M_\odot$ [Bringmann '09, Cornell'12, Gondolo'12]. We use $M_{\text{min}} = 10^{-6} M_\odot$ and although there is significant uncertainty on the order of magnitude of M_{min} , the total deposited energy only depends weakly on it.

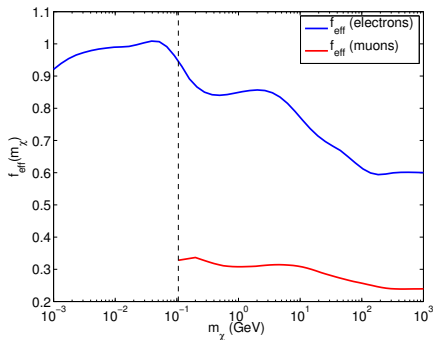
In practice

In order to bypass the computationally expensive interpolation at each redshift of $f(z, m_\chi)$ in our Monte Carlo analyses, we use:

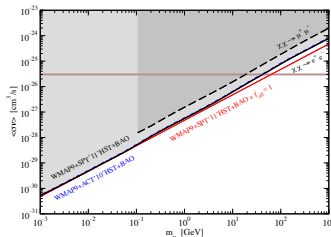
$$\left(\frac{dE}{dt dV} \right)_{\text{deposited}} = (f_{\text{eff}}(m_\chi) + g_{\text{eff}}(z, m_\chi)) \left(\frac{dE}{dt dV} \right)_{\text{injected}} .$$

$$f_{\text{eff}}(m_\chi) = \frac{\int_{z_{\text{max}}}^{z_{\text{min}}} f(z, m_\chi) \sqrt{1+z} dz}{\int_{z_{\text{max}}}^{z_{\text{min}}} \sqrt{1+z} dz} ,$$

$$\text{and } g_{\text{eff}}(z, m_\chi) = \gamma(m_\chi) \Gamma(z)$$



s-wave annihilation results [JCAP 1307 (2013) 046]



Dataset	P_{ann} [$10^{-6} \text{ m}^3 \text{ s}^{-1} \text{ kg}^{-1}$]
WMAP7 + ACT'08 (Galli <i>et al.</i> [21])	< 1.17
WMAP7 + SPT'09 (Giesen <i>et al.</i> [21])	< 0.91
*WMAP7 + SPT'09	< 0.81
WMAP7 + SPT'09	this study
WMAP7 + SPT'09	< 0.64
WMAP9 + SPT'09	< 0.44
WMAP9 <i>only</i>	< 0.66
WMAP7 + SPT'11	< 0.32
WMAP9 + SPT'11	< 0.27
WMAP9 + ACT'10	< 0.29

- Our improved bounds are mainly driven by the better accuracy at high ℓ of the recent ACT and SPT data releases.
- Inclusion of annihilating DM in halos does not modify the exclusion regions. The effects of the halo contribution could only be significant with an enhancement of $g(z, m_\chi)$ of at least two orders of magnitude.
 - An increase of about an order of magnitude could be obtained by using a cusper density profile for the DM halos than NFW.
 - a decrease by four orders of magnitude in the uncertain and model-dependent minimum halo mass ($M_{\text{min}} = 10^{-10} M_\odot$) would increase the maximum value of $g(z, m_\chi)$ only by a modest factor of ~ 2 .

Energy deposition: p-wave annihilation

$$\left(\frac{dE}{dV dt}\right)_{\text{deposited}} = \left[\frac{\langle v^2 \rangle}{v_{\text{ref}}^2} f_p(z, m_\chi) + g_p(z, m_\chi, v_{\text{ref}}) \right] (1+z)^6 \rho_\chi^2 \frac{\sigma v_{\text{ref}}}{m_\chi},$$

$$\bullet \frac{\langle v^2 \rangle}{v_{\text{ref}}^2} = \frac{T_\chi(z)}{T_{\text{ref}}} = \left(\frac{1+z}{1+z_{\text{ref}}} \right)^2.$$

z_{ref} = redshift at which $v_{\text{rms}} \equiv \sqrt{\langle v^2 \rangle}$ of the background DM is equal to v_{ref} . We write it as a function of the redshift of kinetic decoupling z_{KD} corresponding to $T_\chi(z_{\text{KD}}) = T_{\text{KD}}$:
 $1 + z_{\text{ref}} \simeq 2.56 \times 10^7 \left(\frac{T_{\text{KD}}}{\text{MeV}}\right)^{1/2} \left(\frac{m_\chi}{\text{GeV}}\right)^{1/2}.$

- T_{KD} is model dependent, for effective s- or p-wave interactions using [Shoemaker '13]

$$T_{\text{KD}} = 0.69 \frac{g_{\text{eff}}^{1/8}}{g_\chi^{1/4}} \Lambda \left(\frac{48\pi m_\chi}{M_{\text{pl}}} \right)^{1/4} \simeq 2.02 \text{ MeV} \left(\frac{m_\chi}{\text{GeV}} \right)^{3/4}.$$

$$\bullet g_p(z, m_\chi, v_{\text{ref}}) = \frac{H(z)}{(1+z)^3} \sum_i \int E \frac{dN}{dE} dE \sum_i \int dz' \frac{(1+z')^2}{H(z')} G_p(z', v_{\text{ref}}) \int T_i(z', z, E) E \frac{dN}{dE}$$

$$G_p(z, v_{\text{ref}}) \equiv \frac{1}{(\Omega_{\text{DM},0} \rho_{c,0})^2} \frac{1}{(1+z)^6} \int dM \frac{dn(M,z)}{dM} \int_0^{r\Delta} dr 4\pi r^2 \frac{\langle v^2(r) \rangle}{v_{\text{ref}}^2} \rho_{\text{halo}}^2(r).$$

- We assume Maxwell–Boltzmann velocity distrib. : $f(v, \Sigma) = \frac{4\pi}{(2\pi\Sigma^2)^{3/2}} v^2 \exp\left(-\frac{1}{2} \frac{v^2}{\Sigma^2}\right)$,
 $\rightsquigarrow \langle v^2(r) \rangle = 3\Sigma^2(r)$. If we assume hydrostatic equilibrium, the velocity dispersion can be found by integrating the Jeans equation: $\frac{d(\rho\Sigma^2)}{dr} = -\rho \frac{GM(<r)}{r^2}$. This can be done analytically with an NFW profile.

title

This is really the end